

Boosting ORR Kinetics of Protonic Ceramic Fuel Cell via Surface Decoration Using Nonreactive Insulators

Bingbing Qiu^a, Kang Zhu^a, Yi Yang^a, Lujuan Ye^a, Lijie Zhang^a, Changrong Xia^a, Ranran Peng^{a,b,c*} and Yalin Lu^{a,b,c*}

^a Department of Materials Science and Engineering, University of Science and Technology of China, No. 96 Jinzhai Road, Hefei, Anhui Province, 230026, PR China.

^b Synergetic Innovation Center of Quantum Information & Quantum Physics, University of Science and Technology of China, Hefei, Anhui 230026, China.

^c Hefei National Laboratory of Physical Science at the Micro-scale, University of Science and Technology of China, Hefei, 230026 Anhui, China.

*To whom correspondence should be addressed. E-mail: pengrr@ustc.edu.cn and yllu@ustc.edu.cn.

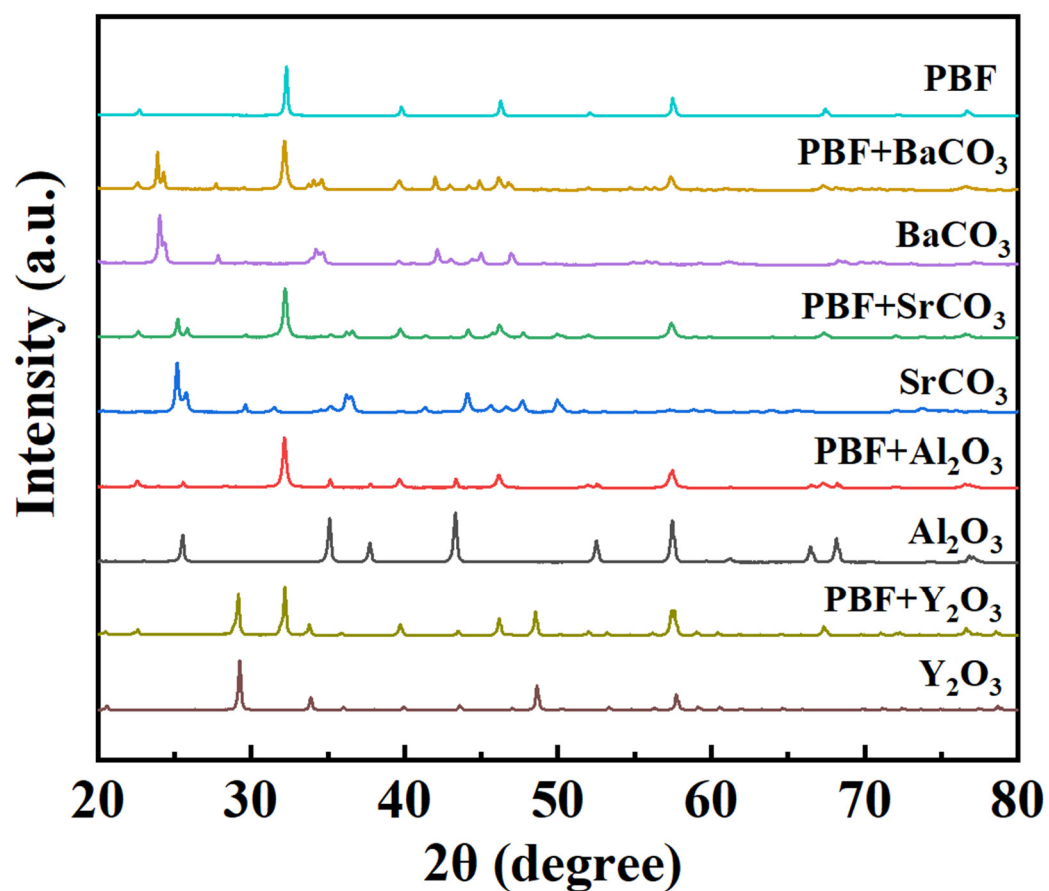


Figure S1 (a) XRD patterns of PBF, insulators, the mixture of PBF and insulators at 1:1 mass ratio and then calcined at 700 °C for 2 h.

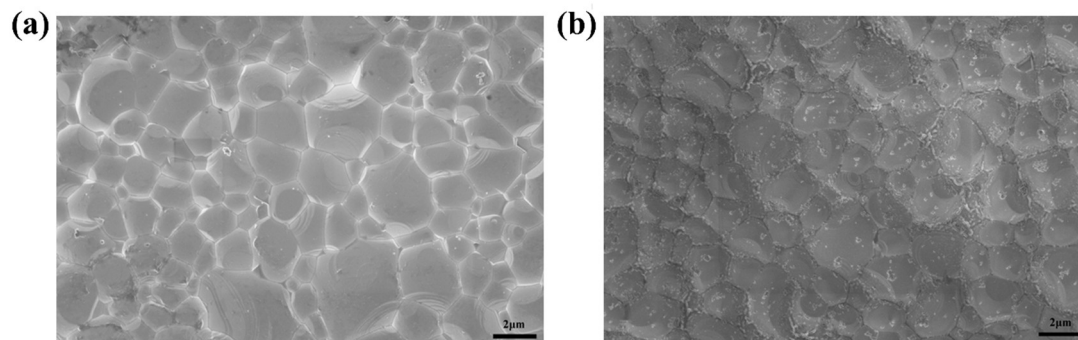


Figure S2 SEM images of surface of dense pristine PBF bars (a) and PBF bars with Y₂O₃.

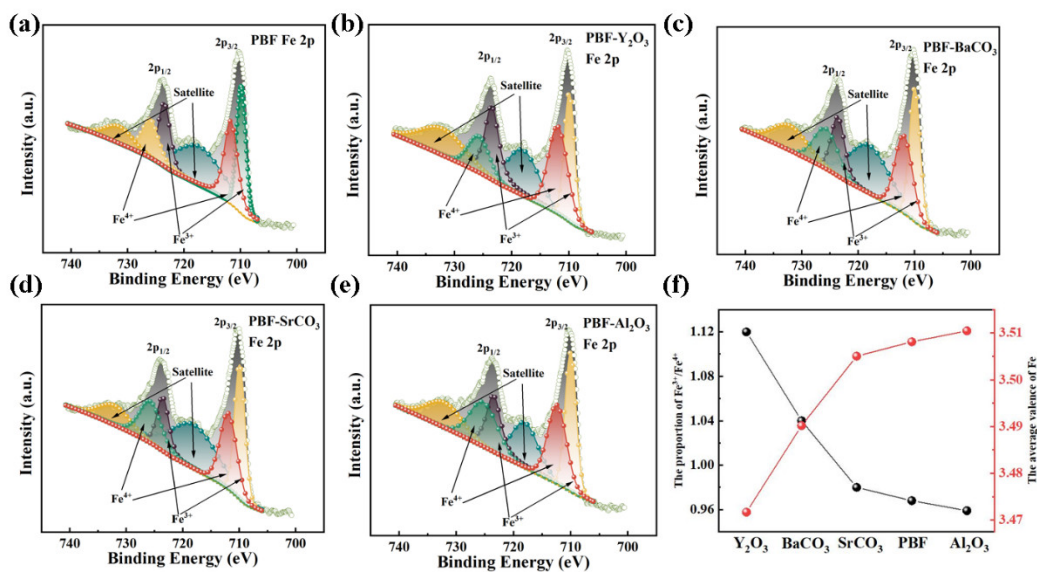


Figure S3 XPS spectra and fitted lines of Fe 2p in the (a)PBF, (b)PBF-Y₂O₃ (c)PBF-BaCO₃, (d)PBF-SrCO₃ and (e)PBF-Al₂O₃ sample at room temperature. (f)The value of Fe³⁺/Fe⁴⁺ and the average valence of Fe.

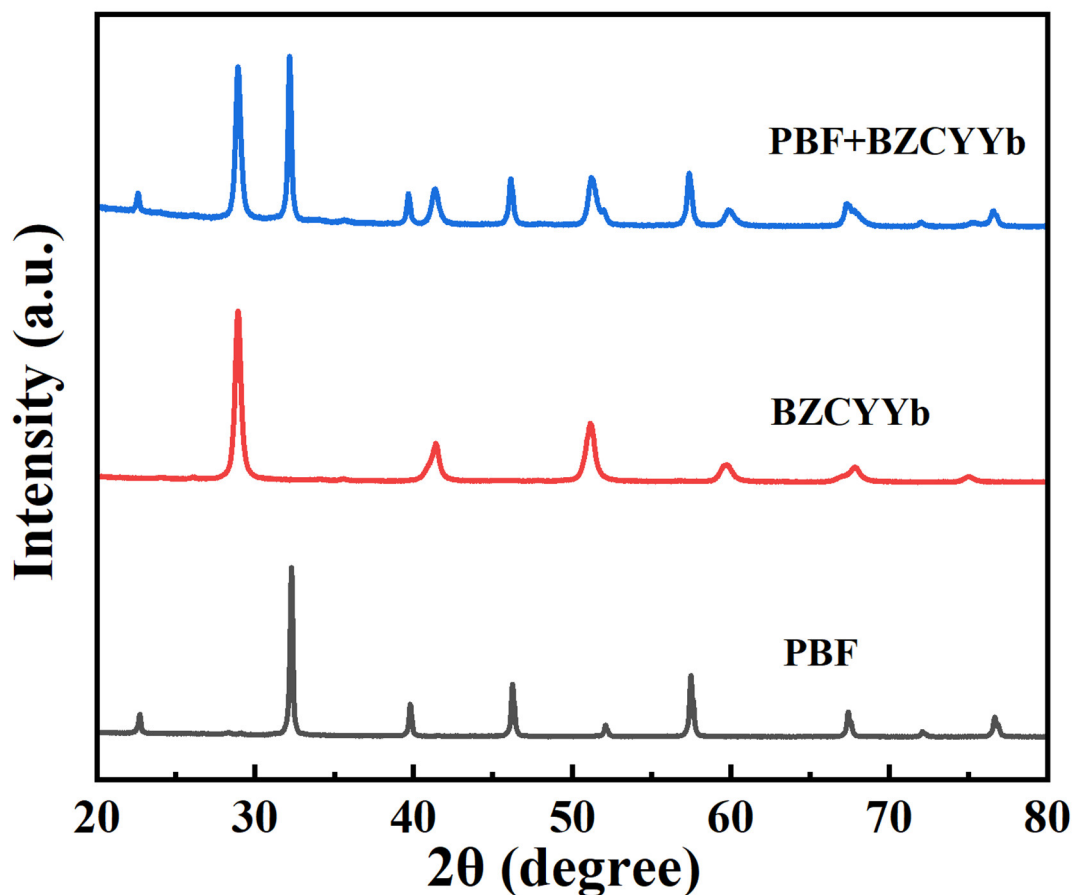


Figure S4 XRD patterns of PBF, BZCYYb, the mixture of PBF and BZCYYb at 1:1 mass ratio and then calcined at 1000 °C for 2 h.

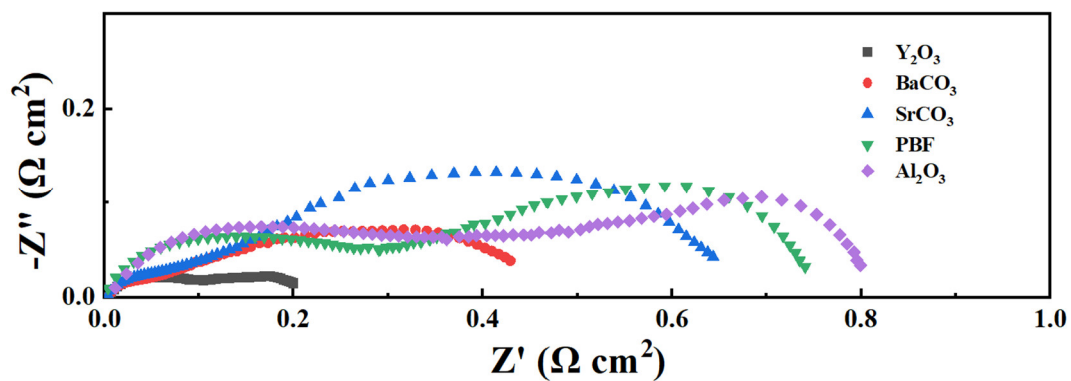


Figure S5 Nyquist impedance plots for PBF and PBF with different insulators at 700 °C.

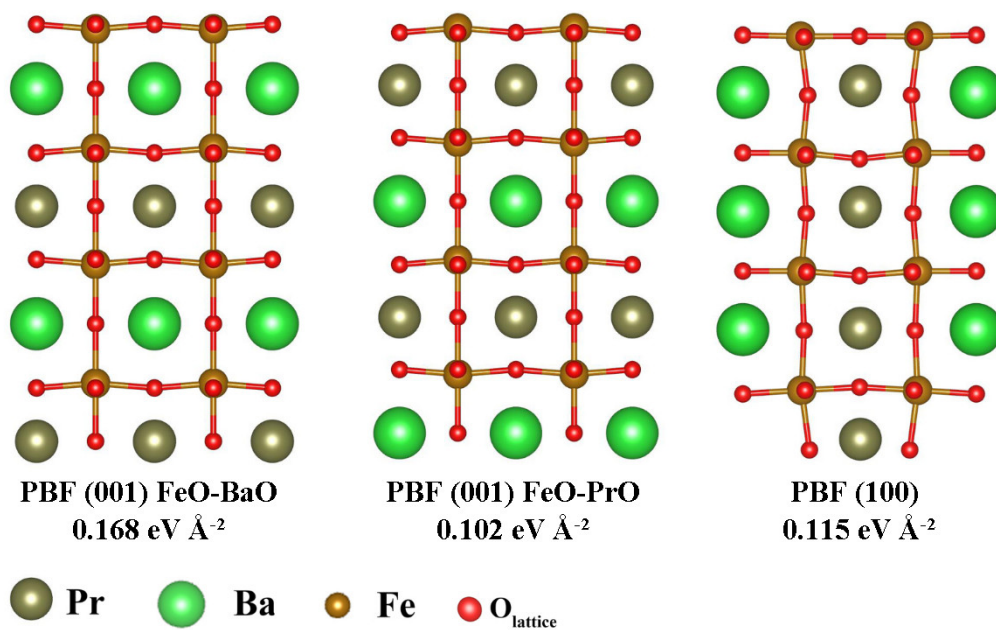


Figure S6 Schematic illustrations of (a) PBF (001) with BaO sub-outer layer (b) PBF(001) with PrO sub- outer layer (c) PBF(100) and their surface energy.

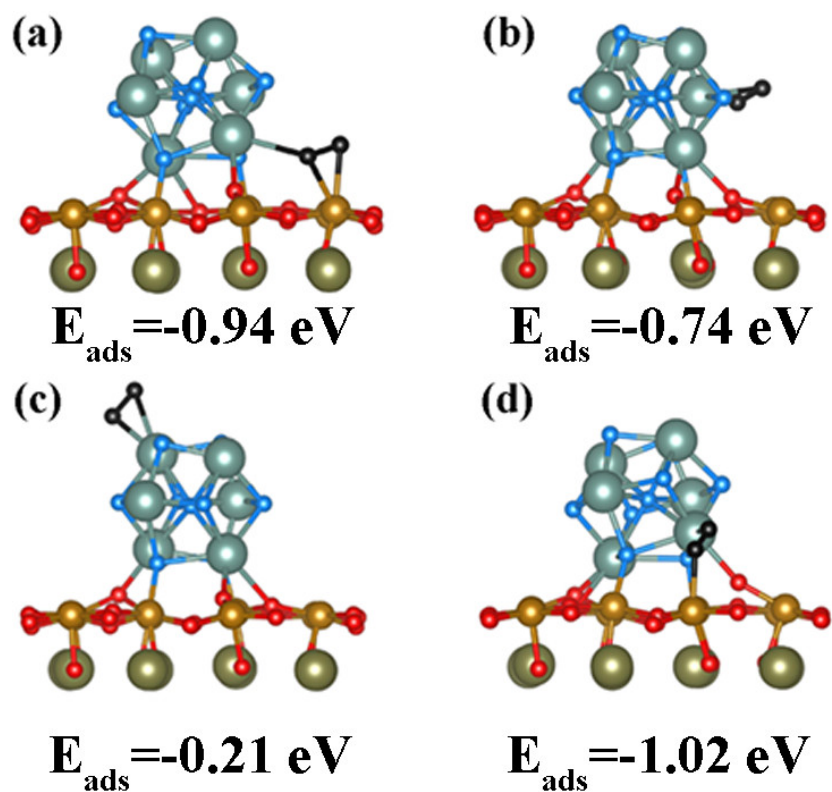


Figure S7 Schematic illustrations of the oxygen absorption structure on PBF with Y_2O_3 surface and the oxygen absorption energy at (a) bottom, (b) middle, (c) top and (d) interface adsorption site.

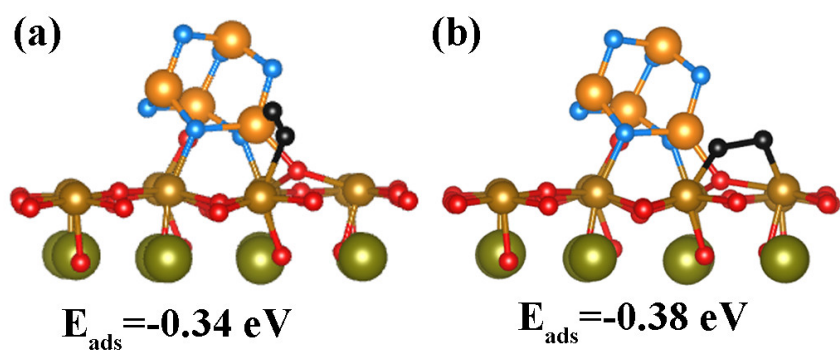


Figure S8 Schematic illustrations of the oxygen absorption structure on PBF with Al_2O_3 surface and the oxygen absorption energy at (a) interface, (b) PBF surface site.

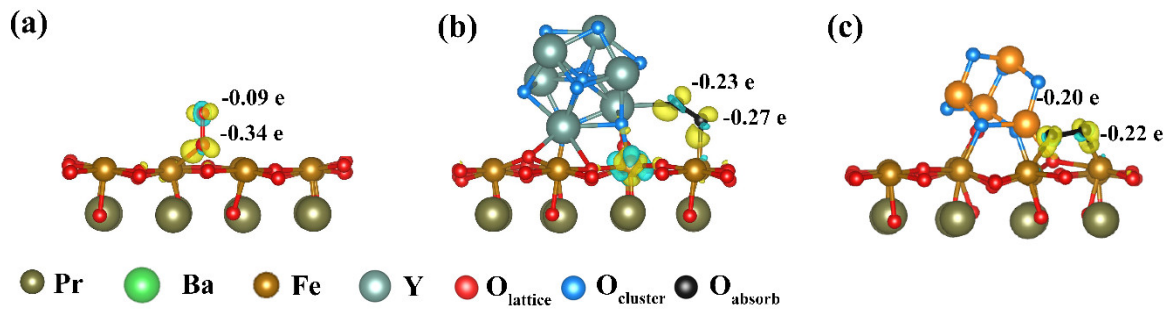


Figure S9 Schematic illustrations and Bader charge analysis of the oxygen absorption structure on (a) bare PBF, (b) PBF with Y_2O_3 surface and (c) PBF with Al_2O_3 surface.

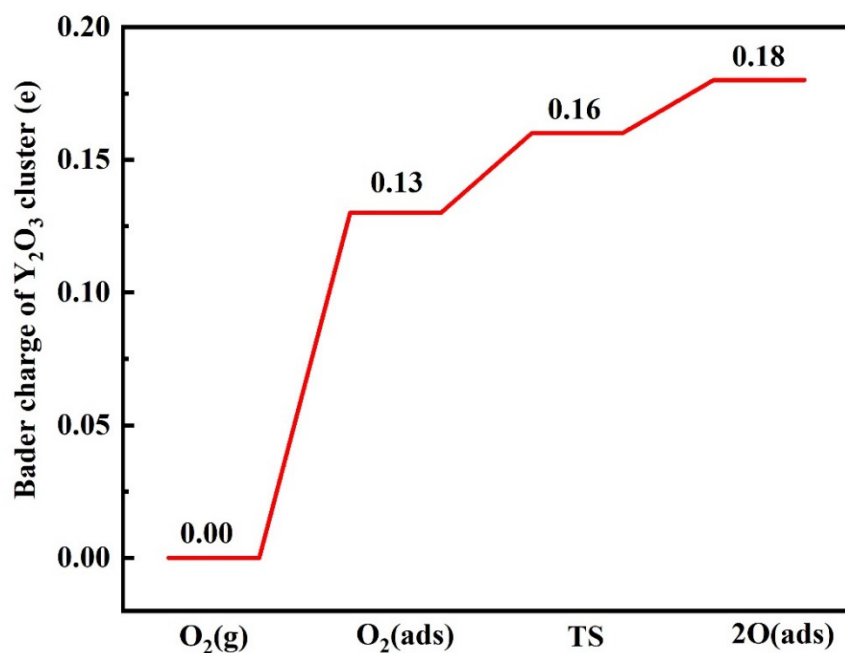


Figure S10 Bader charge of Y_2O_3 cluster during oxygen adsorption and dissociation process.

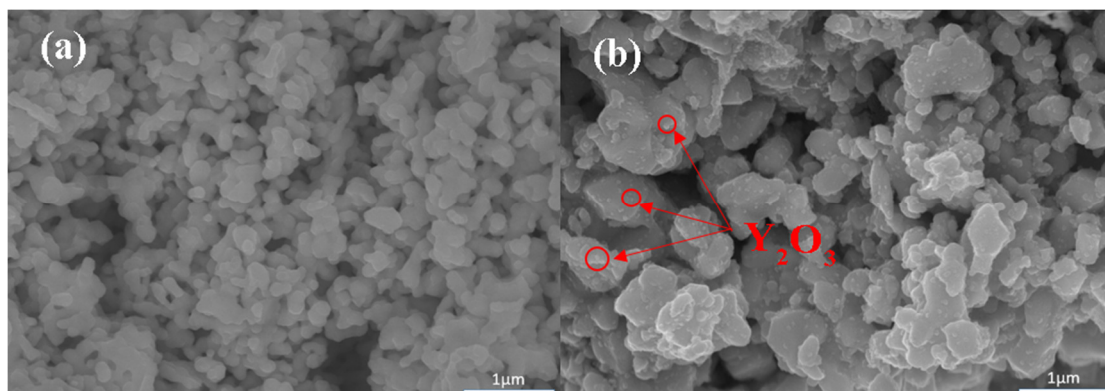


Figure S11 SEM images of (a) pure PBF and (b) PBF with Y_2O_3 nanoparticles.

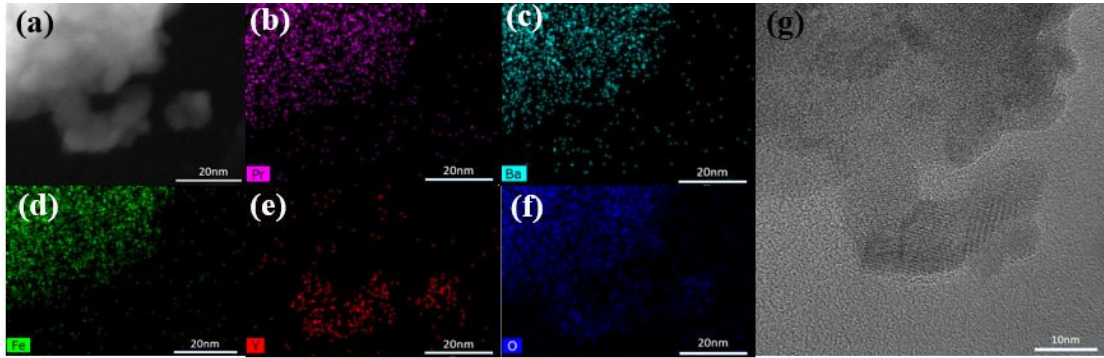


Figure S12 (a)-(f) the EDX mapping and (g) the HRTEM image of the PBF- Y_2O_3 composite cathode.

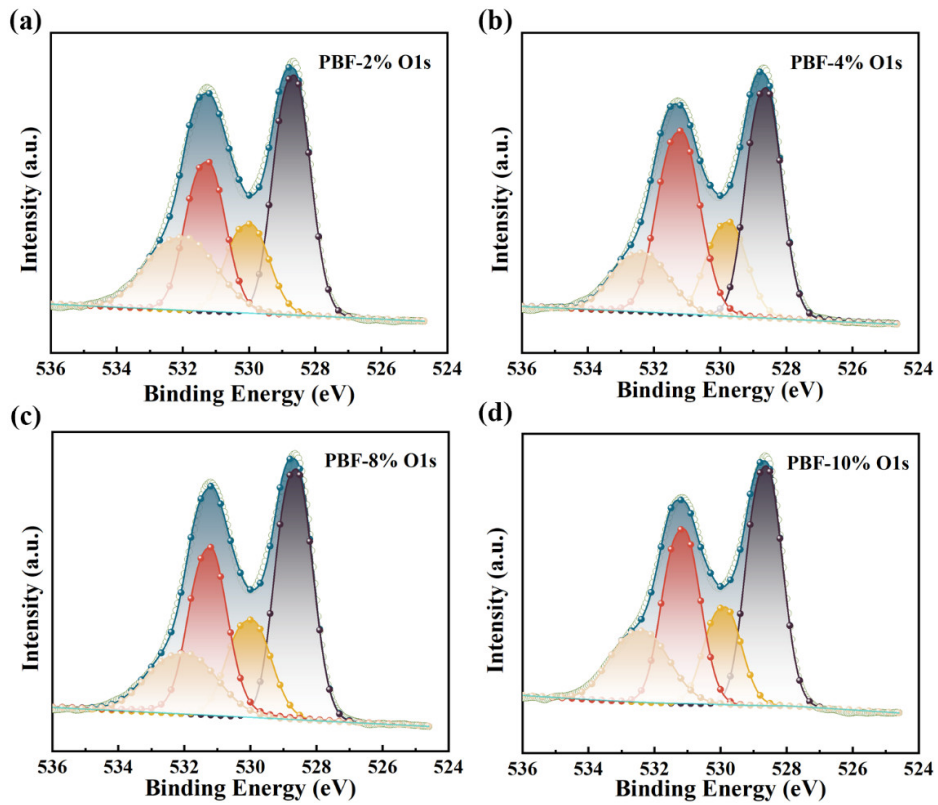


Figure S13 O 1s species on the surface of the PBF with (a) 2%, (b) 4%, (c) 8% and (d) 10% Y_2O_3 .

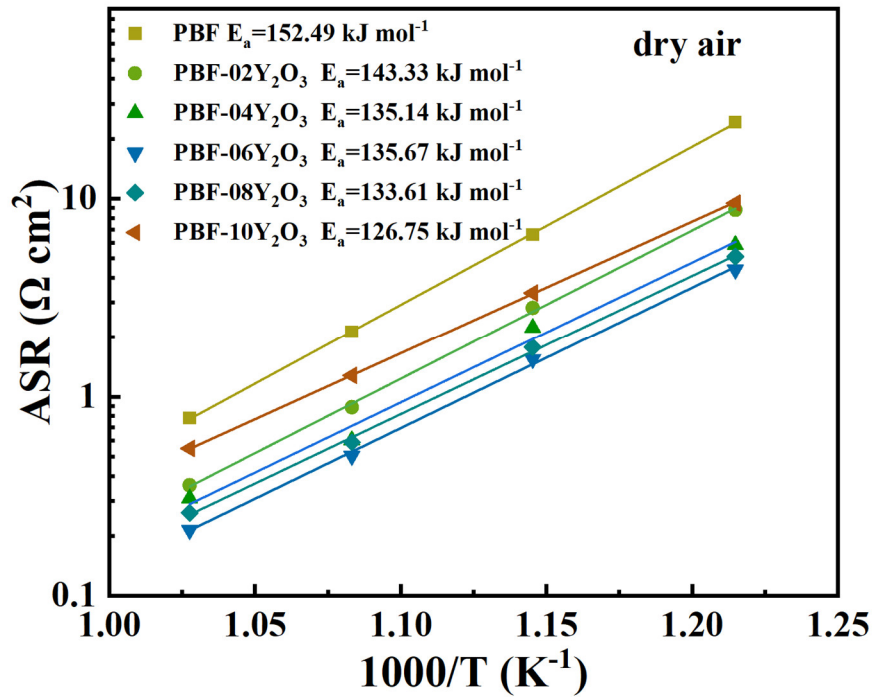


Figure S14 The fitted oxygen surface exchange coefficients and their respective activation energies of PBF and PBF with different amount of Y_2O_3 at 550-700 °C in dry air.

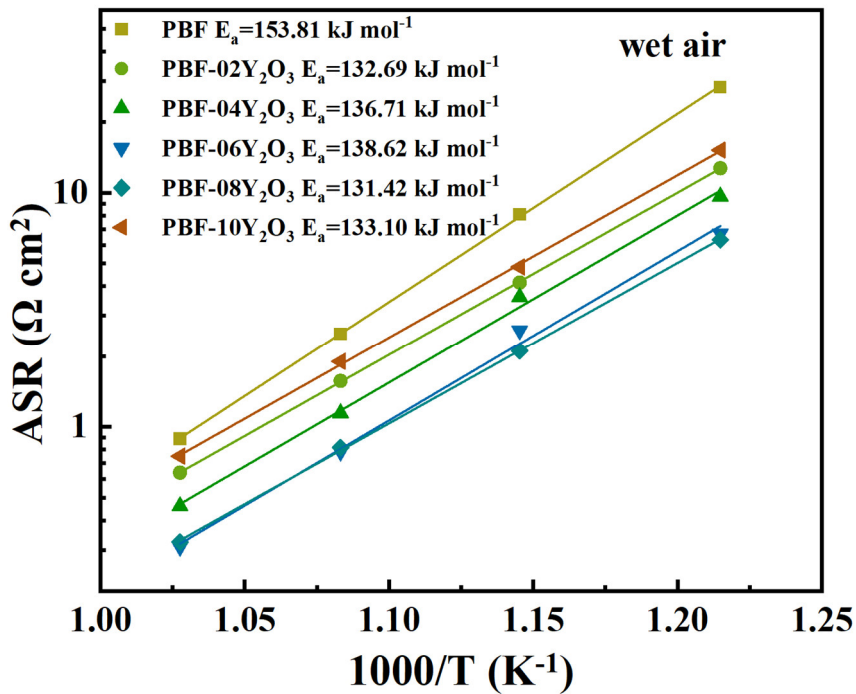


Figure S15 The fitted oxygen surface exchange coefficients and their respective activation energies of PBF and PBF with different amount of Y_2O_3 at 550-700 °C in air containing 3% H_2O .

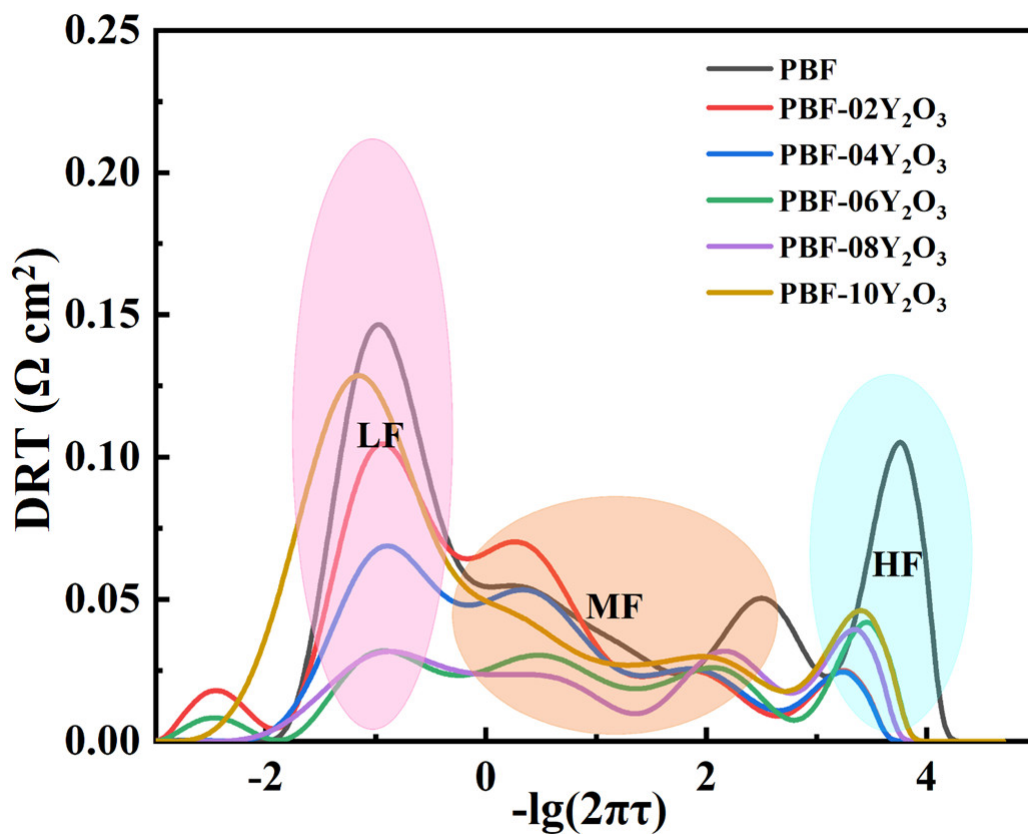


Figure S16 DRT analysis of PBF and PBF with different amount of Y_2O_3 at $700^\circ C$ in wet air.

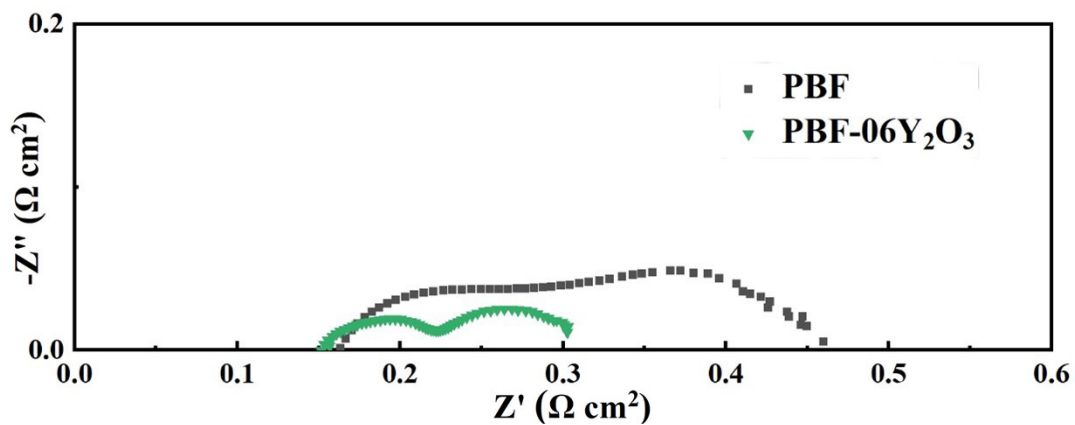


Figure S17 Nyquist impedance plots for single cells with PBF and PBF-06 cathodes.

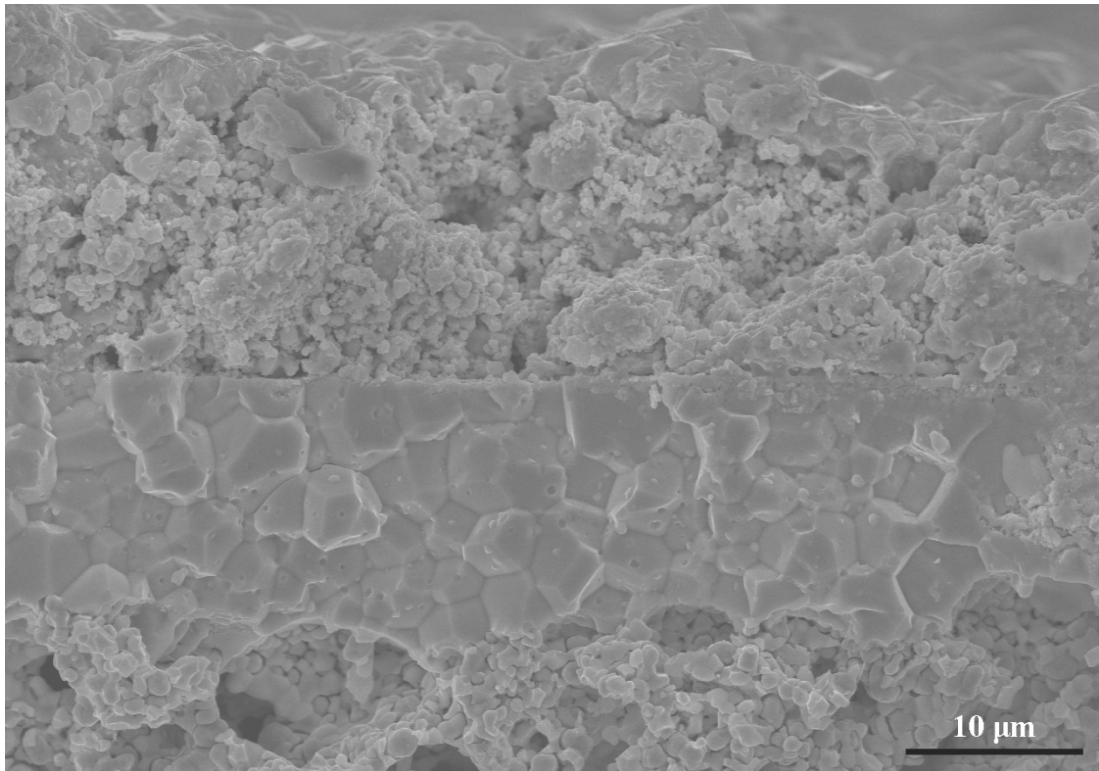


Figure S18 the SEM image of PBF-06Y₂O₃|BZCYYb|Ni-BZCYYb after stability test.